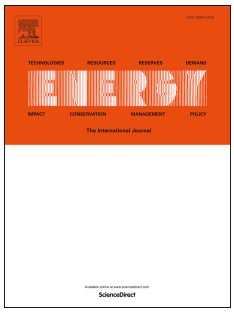

Expandable deep learning for real-time economic generation dispatch and control of three-state energies based future smart grids

Linfei Yin, Qi Gao, Lulin Zhao, Tao Wang

PII: S0360-5442(19)32256-X

DOI: https://doi.org/10.1016/j.energy.2019.116561

Reference: EGY 116561

To appear in: *Energy*

Received Date: 14 May 2019

Revised Date: 3 November 2019

Accepted Date: 14 November 2019

Please cite this article as: Yin L, Gao Q, Zhao L, Wang T, Expandable deep learning for real-time economic generation dispatch and control of three-state energies based future smart grids, *Energy* (2019), doi: https://doi.org/10.1016/j.energy.2019.116561.

Expandable deep learning for real-time economic generation dispatch and control of three-state energies based future smart grids

Linfei Yin[a,*], Qi Gao[a], Lulin Zhao[a], Tao Wang[a]

[a] *College of Electrical Engineering, Guangxi University, Nanning, Guangxi, 530004, China*

Abstract

This paper proposes a three-state energy model, which contains three states, i.e., generator, power load and closed states. Besides, this paper proposes an expandable deep learning for the real-time economic generation dispatch and control of three-state energies based future smart grids. Although three-state energies will interconnected into or disconnected from future smart grids with varying topology, the numbers of inputs and outputs of the proposed expandable deep learning can be expanded dynamically with the varying topology of future smart grids. Since expandable deep learning based real-time economic generation dispatch and controller can simultaneously provide multiple generation commands for future smart grids with varying topology, the framework of conventional generation dispatch and control can be replaced by the real-time economic generation dispatch and control framework. Compared with 216 combined conventional generation dispatch and control algorithms under a 118-bus power system with 54 three-state energies and a 13659-bus power system with a total of 4092 three-state energies in varying topology, the expandable deep learning obtains the highest control performance. Simulation results verify the effectiveness and feasibility of the proposed expandable deep learning for the real-time economic generation dispatch and control of three-state energies based future smart grids with varying number of three-state energies and varying topology.

Keywords: Expandable deep learning; Three-state energies; Real-time economic generation dispatch and control; Web-of-Cells; Unified time scale.

2010 MSC: 00-01, 99-00

1. Introduction

With the applications of numerous renewable energy sources and distributed generation in smart grids or integrated community energy systems [1], the conventional framework of the smart grid contains several deficiencies [2]. The conventional framework of the smart grid contains long time scale optimization and short time scale control [3]. The long time scale optimization and short time scale control could lead to reverse regulation [2]. Therefore, a real-time economic generation dispatch and control (REG) framework has been proposed to replace the conventional generation dispatch and

*Corresponding author

Email address: yinlinfei@163.com (Linfei Yin)

control (CGC) framework in our previous work [2]. This paper is based on the REG framework. However, the relaxed deep learning in the previous work can only be applied into a power system with fixed number of generators and fixed system topology.

However, the numbers of generators and system loads in a real power system are varying numbers. In general, the power load model of electric vehicles is generally regarded as random power loads in current power systems. With the continuous development of spot electricity market [4] and flexible load, the current models of loads and energy sources have one deficiency. For example, the plug-in hybrid electric vehicle (PHEV) [5] can be regarded as three states, i.e., generator [6], power load [7], or closed generator. Numerous schemes for high penetration distributed generations have been studied with wind power, photovoltaic power, and the PHEV [8]. For example, plug-in electric vehicles, wind turbines, photovoltaics, and, fuel cells have been considered in local distribution systems [9]; energy storage has been considered in active distribution networks with wind turbines and photovoltaics [10]; high penetration of wind and solar power have been considered in active distribution networks [11]; high penetration of distributed photovoltaics units have been considered in distribution networks [12]. However, (i) once these high penetration distributed generations are set, the parameters of economic dispatch algorithms and automatic generation controller should be configured fixed; (ii) and, once a new distributed generation is interconnected into the power system, the parameters of economic dispatch (ED) and automatic generation controller should be re-configured once more.

To overcome these deficiencies, this paper proposes three-state energies (TSEs) model for the prosumers, which can be energy producers and energy consumers.

However, the topology of a real power system is varying topology. To control the smart energies of future smart grids, the concept of Web-of-Cells (WoCs) has been proposed by the *European Liaison on Electricity Committed Towards long-term Research Activities* Integrated Research Programme on Smart Grids brings [13]. The intelligent dispatch and control framework of the WoCs should has the abilities of self-organization coupling and autonomous learning [14]. In the framework of WoCs, the future smart grid is connected by multiple subsystems, which are the cells of the WoCs. Each subsystem is connected by various prosumers, which are the subsidiary cells of the cells of the WoCs. Therefore, (1) the cells of the WoCs can be subsystems or prosumers; (2) a future smart grid is connected by numerous prosumers. Since a prosumer can interconnected into or disconnected from the WoCs at any time, the topology of the WoCs in future smart grids with numerous renewable energy sources is a varying topology [15]. The conventional ED [16] and automatic generation control (AGC) algorithms [17] are difficult to adapt the expandable future smart grids with varying topology [18, 19]. Conventional ED algorithms provide generation commands for generators with the prediction of system load at every 15 minutes [20]. Conventional AGC controllers provide real-time generation commands for generators with the system load disturbance [21]. Consequently, a CGC controller is difficult to provide control commands for the prosumers of the WoCs [22].

The optimization and control algorithms with fixed energy producers and fixed energy consumers could not solve the optimization and control problems of future smart grids based on WoCs with varying topology. To solve the optimization and control problem of an expandable future smart grids with

TSEs, this paper proposes an expandable deep learning (EDL) algorithm for future smart grids based on WoCs. The EDL based REG framework is designed to replace the CGC framework, which contains four processes, i.e., unit commitment (UC) [23], ED [24], AGC, and generation command dispatch (GCD) [25]. Generally, the period of the optimization algorithms for the UC of smart grids is 1 day or 24 hours [26]; the period of the optimization algorithms for the ED of smart grids can be set to 4 hours, 1 hour, or 15 minutes [27]. The deficiencies of the CGC framework with multiple time scales should be mitigated by the EDL based REG controller with unified time scale.

A total of 216 combined CGC algorithms are compared with the EDL based REG controller in this paper. The major features of the proposed EDL can be summarized as follows,

(1) Since the numbers of inputs and outputs of the EDL can be expanded, the numbers of inputs and outputs of the EDL based controller can be increased or decreased with varying topology.
(2) Multiple three-state energies can be controlled by the EDL based controller with the ability of multiple outputs.

Therefore, the major contributions of this work can be summarized as follows,

(1) Since the three-state energy model is built for future smart grids, all the nodes of the future smart grid can be three-state energies, such as wind power, photovoltaic power, energy storage, and PHEVs.
(2) One node of the future smart grid can be energy at current time, and the node can be system load at next time. Furthermore, all the nodes of the future smart grid with three-state can be controlled by the proposed approach in this paper.
(3) Since the energies or system load can be interconnected into and disconnected from the future smart grid at any time in the future, the number of three-state energies will be a varying number in the future. Then, the framework of the future smart grid at the next time will be different with the framework at current time. The energies and system load of the future smart grid with varying framework can be controlled by the EDL based REG controller.

The remaining of this paper is organized as follows. The models of the CGC and the algorithms for CGC are analyzed in Section 2. The REG framework is developed in Section 3. Section 4 describes the basic principle of the proposed EDL algorithm. Simulation results are presented in Section 5. Section 6 briefly concludes this paper.

2. Framework of conventional generation dispatch and control

2.1. Models of conventional generation dispatch and control

Although the CGC framework contains four processes (Fig. 1), each generation unit can only obtain one generation command from the AGC controller in each iteration [2].

The major features of a conventional power system:

(1) Each UC programming, which provides the states $u_{j,t}$ and active power $P_{j,t}$ for the j-th generator (or generation unit) at the time of t, should be finished in 24 hours.

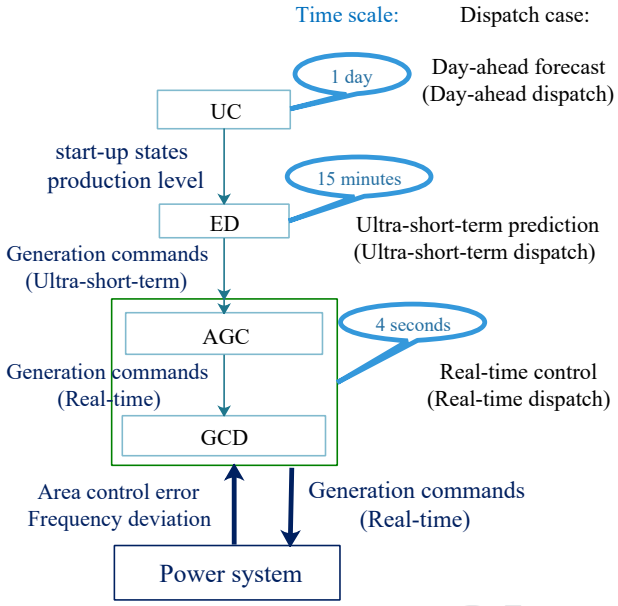

Fig. 1. Model of conventional generation dispatch and control with time scales

Table 1. Inputs and outputs of conventional generation dispatch and control framework

Process	Type of algorithm	Time slot	Inputs	Outputs
UC	Optimization algorithm	24 hours	Predicted load $PD_{i,t}$	States $u_{i,j,t}$, generation command $P_{j,t}$
ED	Optimization algorithm	15 minutes	Predicted load PD_i	Generation command $P_{i,j}$
AGC	Control algorithm	4 s	Area control error e_i, frequency deviation Δf_i	Increment generation command ΔP_i
GCD	Optimization algorithm	4 s	Increment generation command ΔP_i	Increment generation command $\Delta P_{i,j}$

(2) Each ED programming, which provides the active power of the j-th generating unit P_j, should be finished in 15 minutes in this paper.

(3) The total calculation time of AGC and GCD programming should be less than 4 s. From the time scale perspective, AGC programming should provide generation command P_j for the j-th generator in each 4 s.

2.2. Algorithms for conventional generation dispatch and control framework

In the CGC framework, the AGC is solved by control algorithms; while the UC, the ED, and the GCD problems are solved by optimization algorithms [2]. A total of 26 optimization algorithms are simulated for the UC, the ED, and the GCD problems, such as simulated annealing algorithm [28], multi-verse optimizer [29], particle swarm optimization [30], imperialist competitive algorithm [31], biogeography-based optimization [32], shuffled complex evolution [33], firefly algorithm [34], cultural algorithm [35], and shuffled frog leaping algorithm [36]. A total of 8 control algorithms are simulated for the AGC problem, such as proportional-integral-derivative (PID), fuzzy logic control [37], fractional order PID [38], active disturbance rejection control [39], Q learning, Q(λ) learning, and R(λ) learning [40]. Table 1 shows the inputs and the outputs of the four processes of the CGC framework.

3. Framework of real-time economic generation dispatch and control

The future smart grids based on the concept of the WoCs consist of numerous prosumers, which are based on three-state energy model. The dispatch and control framework of future smart grids is based on the REG framework. Each prosumer of future smart grids is controlled by a unified energy controller, which is designed in this paper.

3.1. Three-state energy model of future smart grids

A flexible prosumer in future smart grids has flexibility forms, such as energy producer and energy consumer. Therefore, the prosumer of power systems has three states, i.e., generation state, load state, and closed generator state. The prosumer with the generation state of TSEs is an energy producer. The prosumer with the load state of TSEs is an energy consumer. The prosumer with the closed generator state of TSEs is an off-line energy source or load; and this prosumer could be interconnected into future smart grids at any time. Since the state of a prosumer can be one state of these three states at any time, the TSEs is proposed to describe the prosumers. The generation of one three-state energy (TSE) can be small hydro power, wind power, photovoltaic power, micro gas turbine, fuel cells, biomass generator, diesel generator, or flywheel energy storage system. These generators can be regulated by generation commands in future smart grids. The loads of one TSE can be conventional inflexible load or flexible load, which can be controlled by an operator. The TSE with closed state can be closed generation or load, and they have no power flow. Furthermore, one TSE can be generation at one time, and can be load at another time. For example, a PHEV can be a generator when the price of the future smart grids is high, and it can be load when the price of the future smart grids is low (Fig. 2).

Therefore, the future smart grid consists of various prosumers. In the TSEs based future smart grids: the generation state of the TSEs means the producer of prosumers; the load state of the TSEs means the consumer of prosumers; the closed generator state of the TSEs means the off-line producer or the off-line consumer of prosumers.

3.2. Model of real-time economic generation dispatch and control

The control schemes of generation control for future smart grids based on the concept of WoCs has been divided to three steering control time scales, i.e., adaptive frequency containment control, balance restoration control, and balance steering control. However, the framework of REG is applied into future smart grids with unified time scale in this paper (Fig. 3).

Since the REG controller is a multi-output controller, the REG controller can replace the CGC controller [2]. While the output of the REG controller has at least five control modes:

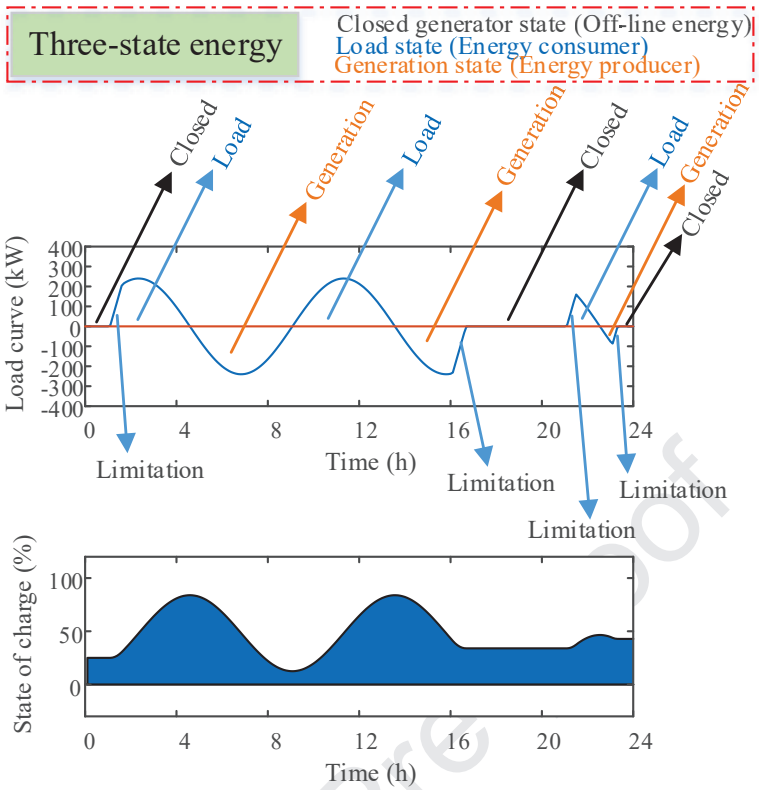

Fig. 2. Load curve of one three-state energy

1. AGC unit mode: the output of the REG controller is a generation command if the TSE is an AGC unit;
2. Distribution mode: the output of the REG controller is the controllable maximum output if the TSE is a wind power or photovoltaic power;
3. Flexible load model: the output of the REG controller is the controllable minimum output if the TSE is a flexible load;
4. Inflexible load mode: the output of the REG controller is not work if the TSE is an inflexible load;
5. Prosumer mode: the output of the REG controller is the controllable output if the TSE is a plug-in hybrid electric vehicle.

Furthermore, the control mode of one TSE is a varying control mode. For example, one TSE can be the distribution mode at the current time; while the TSE can be the prosumer mode at the next time.

3.3. Unified energy controller for real-time economic generation dispatch and control

Any state of the three states of a TSE can be converted with each other. All the states of the TSEs can be controlled by a unified energy controller, which can be regard as a hardware implementation of "energy hub" [41]. The unified energy controller then sends a generation command to the TSE by

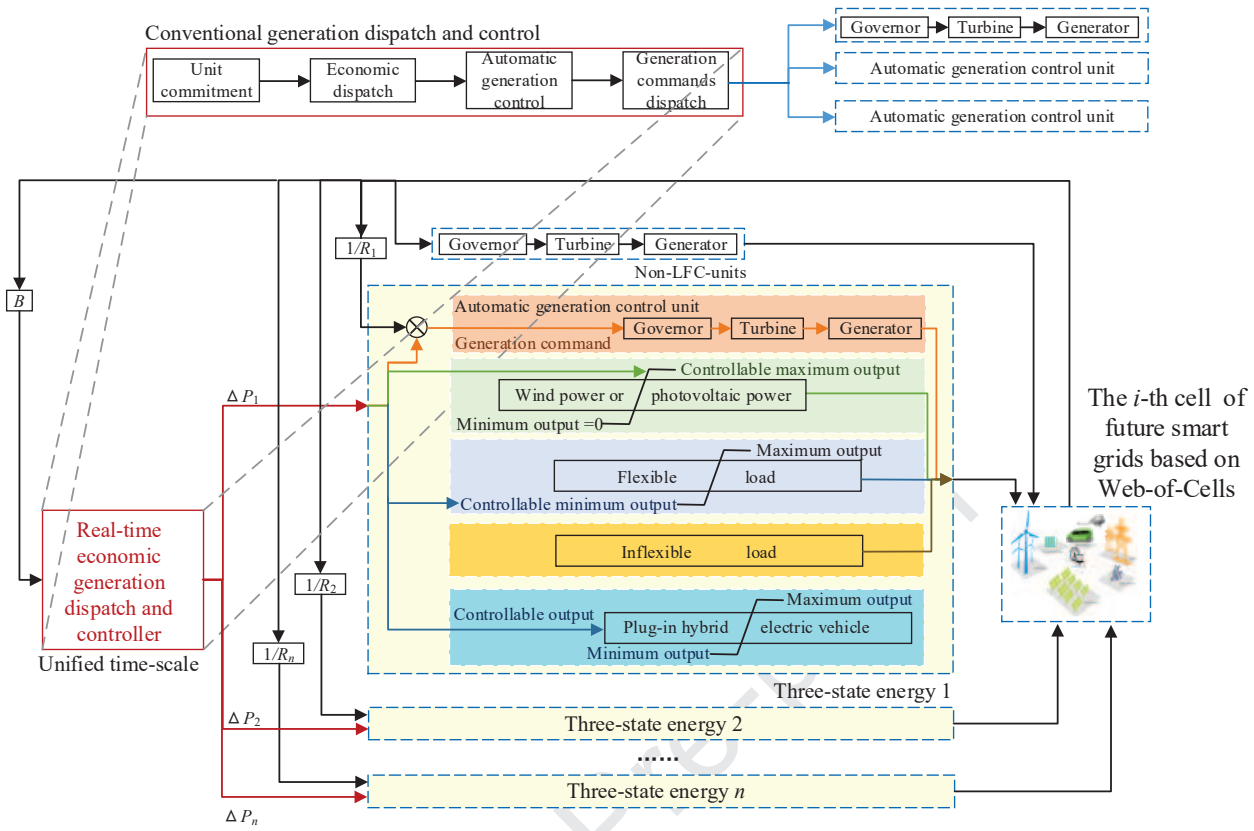

Fig. 3. Framework of real-time economic generation dispatch and control

wireless fidelity (Wi-Fi), Zigbee, or power line communication (PLC). Therefore, any type of TSE can receive the generation command by homologous devices in the future smart grids, such as Wi-Fi module, Zigbee module, and PLC module. Similar to the TSEs of future smart grids, the TSEs of additional smart grids can be controlled by the generation commands. While in the stock smart grids, numerous devices should be improved.

The designed unified energy controller consists of a digital signal processor (DSP) board and an advanced RISC machine (ARM) board. The DSP board communicates with ARM board by serial port. The unified energy controller can be set to numerous controlled modes, for example, controllable generation mode, inflexible load mode, flexible load mode, and controllable prosumer mode (Fig. 3). These modes can be set by the android application in the ARM board. The unified energy controller can receive the generation commands from the REG controller with TCP/IP protocol. Both real-time voltage and current of a TSE can be detected by the DSP board, and these real-time voltage and current values can be showed in the Android application (Fig. 4).

The DSP board of the unified energy controller contains DSP, network terminal, serial port, debug port, temperate transformer, humidity transformer, Zigbee port, three air-break switches, relay, connecting terminal, current transformer. The DSP is a microprocessor control unit for the DSP

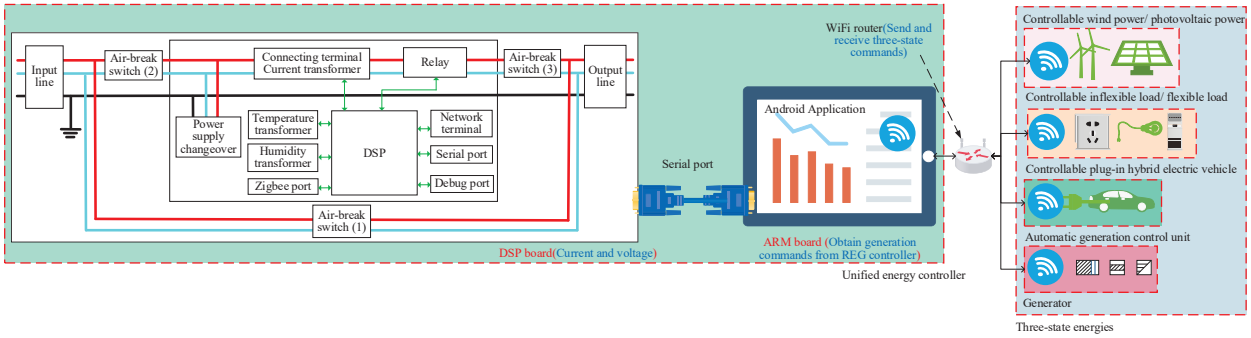

Fig. 4. Structure of unified energy controller

board; the network terminal is an alternative solution for the Wi-Fi module. The left serial port (Fig. 4) is an alternative interface for the parameter regulation. The temperature transformer and humidity transformer are applied to monitor the transformer and humidity of the current environment. The unified energy controller is not working if the 'air-break switch 1' is switched on. The unified energy controller is not powered off if the 'air-break switch 2' is switched off. The output of the unified energy controller is powered off if the 'air-break switch 3' is switched off.

The ARM board of the unified energy controller contains a Wi-Fi module and a serial port. The TSE receive the generation commands from the ARM board by a Wi-Fi router. And these generation commands are received by the DSP board from the REG controller. The power information (i.e., the value of current and voltage) is sent to the REG controller by the ARM board of the unified energy controller.

4. Expandable deep learning for real-time economic generation dispatch and control

The future smart grid based on the concept of WoCs contains numerous cells, and the unified energy controllers of each cell can obtain generation commands from the REG controller of its cell. The outputs of each REG controller are provided by the proposed EDL algorithm. The EDL based REG controller should be pre-trained before the unified energy controller are applied in the WoCs.

4.1. Basic principle of expandable deep learning

An EDL is proposed for dynamic expandable future smart grids in this paper. The major difference between the proposed EDL and dynamically expandable networks (DENs) can be summarized as follows: the EDL is applied to dynamically expand the number of outputs and the number of inputs, while the DENs method was applied to increase the capacity of the networks [42].

The proposed EDL consists of expanding operation and basic deep learning. The basic deep learning of the EDL is based on deep neural networks [2]. The expanding operation of the EDL is depended on

the varying of the numbers of the inputs or the outputs (Fig. 5). The numbers of the hidden units of the first hidden layer and last hidden layer should be larger than the numbers of the inputs and outputs, respectively. Consequently, the number of layers should be larger than 3 in the EDL. The numbers of hidden units of the second layer should be larger than the numbers of the inputs and the outputs. For example, the numbers of the hidden units of the hidden layers of a deep neural network can be set to

$$[n_1 n_{\mathrm{i}}, n_2 n_{\mathrm{i}}, n_3 n_{\mathrm{o}}, n_4 n_{\mathrm{o}}] \tag{1}$$

where n_{i} and n_{o} are the numbers of the inputs and the outputs of the deep neural network, respectively; all the variables n_1, n_2, n_3, and n_4 are the coefficients of the hidden units of the EDL. The numbers of the hidden units can be expanded to

$$[n_1(1+n_{\mathrm{i}}), n_2(1+n_{\mathrm{i}}), n_3 n_{\mathrm{o}}, n_4 n_{\mathrm{o}}] \tag{2}$$

when the number of the inputs of the EDL is added. Then, the information of the cells is added in the future smart grid. Besides, the numbers of the hidden units can be expanded to

$$[n_1 n_{\mathrm{i}}, n_2 n_{\mathrm{i}}, n_3(1+n_{\mathrm{o}}), n_4(1+n_{\mathrm{o}})] \tag{3}$$

when the number of the outputs of the EDL is added. Then, the number of TSEs of a cell is added in the future smart grid. Therefore, the number of the hidden units can be expanded to

$$[n_1(n_{\mathrm{i}}^{'}+n_{\mathrm{i}}), n_2(n_{\mathrm{i}}^{'}+n_{\mathrm{i}}), n_3(n_{\mathrm{o}}^{'}+n_{\mathrm{o}}), n_4(n_{\mathrm{o}}^{'}+n_{\mathrm{o}})] \tag{4}$$

when both numbers of the inputs and the outputs of the EDL are added to $(n_{\mathrm{i}}^{'}+n_{\mathrm{i}})$ and $(n_{\mathrm{o}}^{'}+n_{\mathrm{o}})$, respectively.

The future smart grids have two major flexible features:

1. The grids of the TSEs in future smart grids are varying grids, especial in the case of that numerous TSEs are closed (off-line prosumers).
2. The control mode of the TSE is a varying model. Thus, the output of the EDL based REG controller may not work if the control mode of the TSE is inflexible load mode.

The EDL based REG controller, which is a multi-output controller with expandable ability, can satisfy these two flexible features. The inputs of the i-th REG controller based on the EDL are the information of the i-th cell, i.e., the frequency deviation of the i-th cell Δf_i, and the cell control error (CCE) between the i-th cell and the others e_i. The outputs of the i-th REG controller based on the

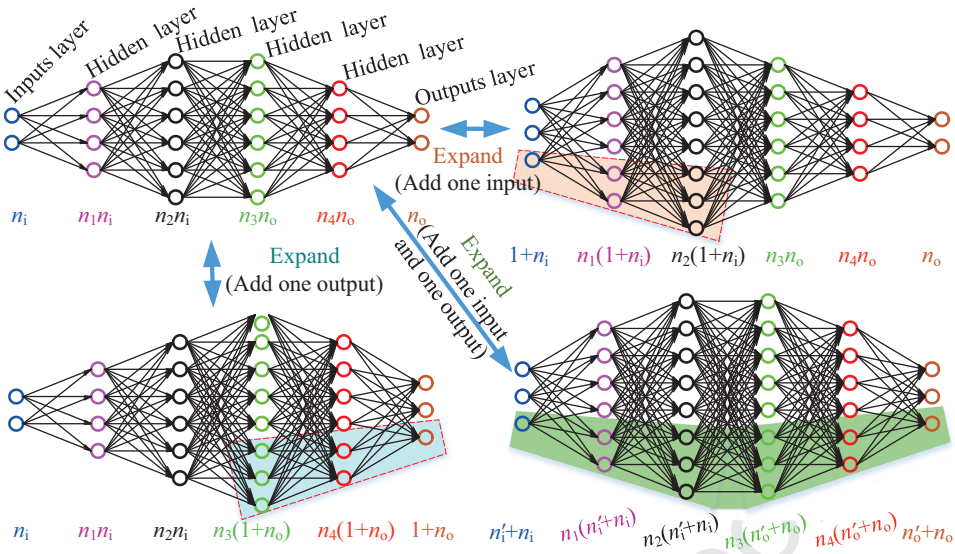

Fig. 5. Expand process of expandable deep learning

EDL are three-state commands for the TSEs of the i-th cell $\{\Delta P_{i,1}, \Delta P_{i,2}, ..., \Delta P_{i,c_i}\}$ (Fig. 6), where c_i is the number of the TSEs of the i-th cell. Therefore, the number of inputs of the EDL n_i is equal to the sum of the number frequency deviation Δf_i and the number of CCE e_i; the number of outputs of the EDL n_o is equal to the number of the TSEs based prosumers. The coefficients n_1, n_2, n_3, and n_4 should be configured for a real application. Since the CCE is similar to the area control error of the CGC framework, the number of cells c_i in future smart grids is similar to the number of areas in the CGC framework.

After the current frequency deviation Δf_i and CCE e_i are obtained by the controller, the deep neural network of the EDL controller should be expanded if the number of the information or the TSEs has been varied (Fig. 6). And the parameters of the expanded hidden units then should be initialized. The next information of the cell, i.e., $\Delta F_i^{'}$, can be predicted by the EDL. The optimal action vector A_k can be selected from the k-th column of an actions set A, while the $\Delta f_{i,k}^{'}$ is the minimum frequency deviation. The initialization of the actions set A is generated as,

$$A = \begin{bmatrix} a_{1,1} & a_{1,2} & \cdots & a_{1,c_i} \\ a_{2,1} & a_{2,2} & \cdots & a_{2,c_i} \\ \vdots & \vdots & \ddots & \vdots \\ a_{n_{\mathrm{a}},1} & a_{n_{\mathrm{a}},2} & \cdots & a_{n_{\mathrm{a}},c_i} \end{bmatrix} \tag{5}$$

where A has c_i columns, and each column is a three-state command vector of actions for a TSE; n_{a} is the number of configured action vectors. Therefore, actions set A is an active power command set for the prosumers of future smart grids. The selected action vector A_k can be relaxed by the relaxed

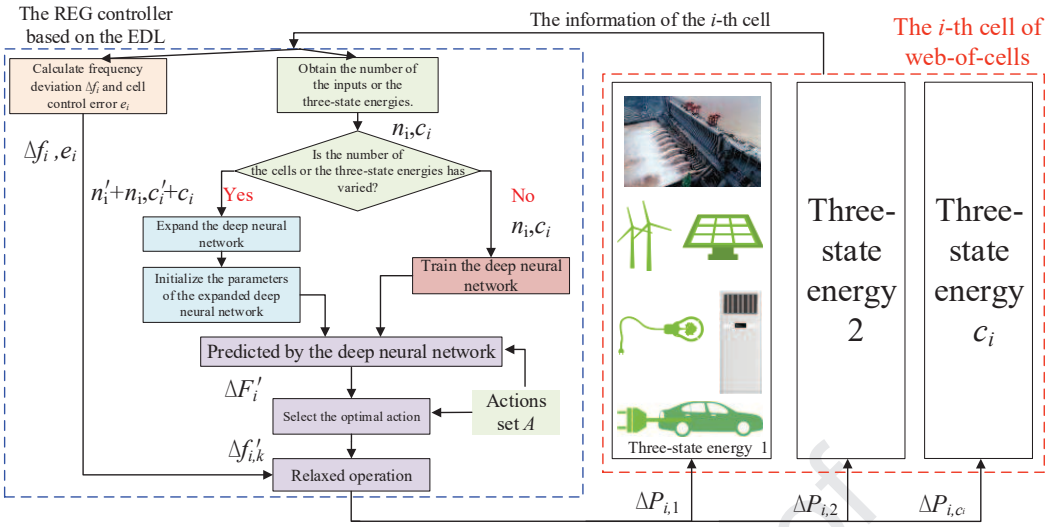

Fig. 6. Flow chart of expandable deep learning based real-time economic generation dispatch and controller

operation for the constraint of the TSEs of the i-th cell. Consequently, the constraint for the relaxed operation can be described as follows [2],

$$\Delta P_{i,j} = \frac{r\left(\Delta P_{i,j} u_{j,t}^{'}\right) \sum_{k=1}^{c_i} \left(\Delta P_{i,k}\right)}{\sum_{k=1}^{c_i} \left(r\left(\Delta P_{i,k} u_{j,t}^{'}\right)\right)} \tag{6}$$

where the constraint function $r\left(\Delta P_{i,j} u_{j,t}^{'}\right)$ is calculated as follows [2],

$$\max\left\{P_{j,(t-1)} - P_j^{\text{down}}, u_{j,t}^{'} P_j^{\min}\right\} \le \Delta P_{i,j} u_{j,t}^{'} \le \min\left\{P_{j,(t-1)} + P_j^{\text{up}}, u_{j,t}^{'} P_j^{\max}\right\} \tag{7}$$

where the temporary start-up state $u_{j,t}^{'}$ can be updated as follows [2],

$$u_{j,t}^{'} = \begin{cases} 1, \ [\Delta P_{i,j}] > 0 \text{ or } 1 \le T_{j,(t-1)}^{\text{up}} < T_j^{\text{min-up}} \\ 0, \ [\Delta P_{i,j}] = 0 \text{ or } 1 \le T_{j,(t-1)}^{\text{down}} < T_j^{\text{min-down}} \end{cases} \tag{8}$$

With the relaxed operation is considered in the EDL, both the upper boundary and the lower boundary of the outputs are bounded. Therefore, the TSEs based prosumers of future smart grids can be controlled by the EDL based REG controller in safety.

4.2. Pre-training process of expandable deep learning

The outputs of each EDL based REG controller are three-state commands for the cells of future smart grids, i.e., generation command, load command, closed command. The inputs of each REG controller based on the deep neural network are the information of the i-th cell and actions vector, i.e., frequency

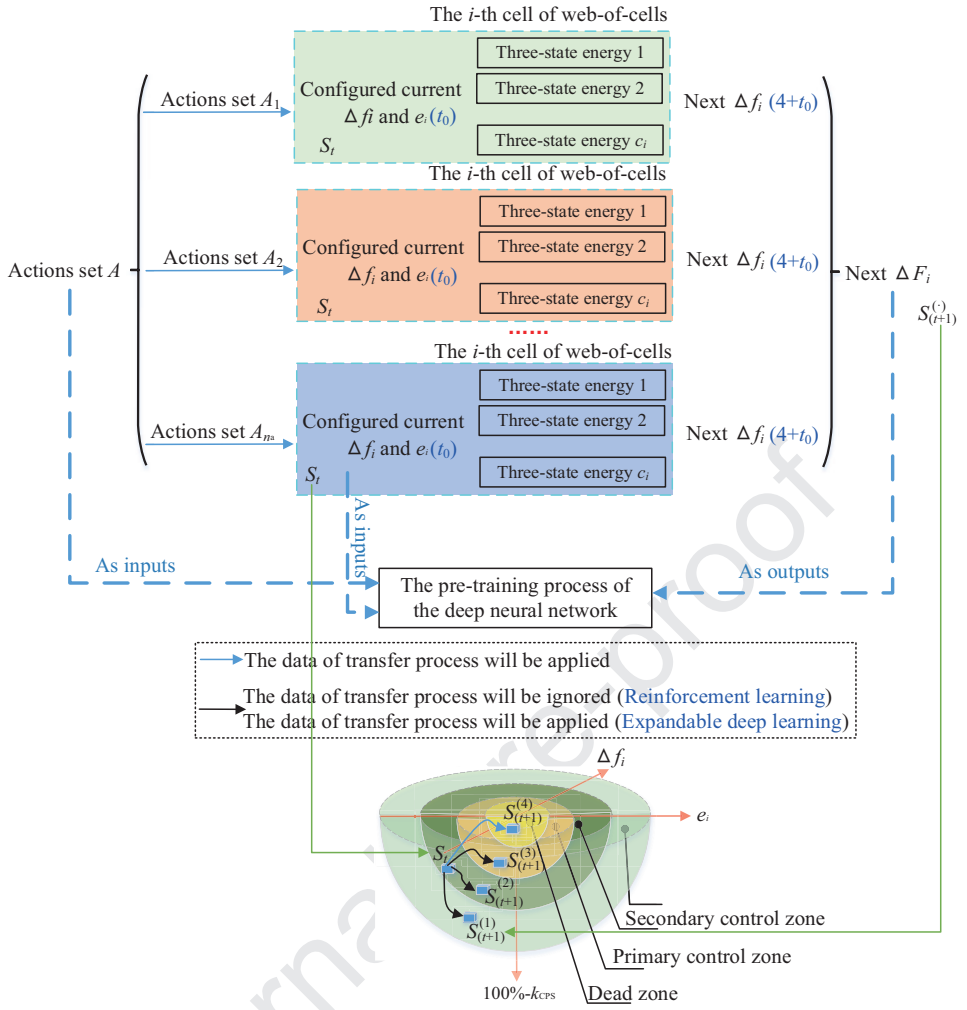

Fig. 7. Pre-training process of expandable deep learning

deviation Δf_i, CCE e_i, and actions vector A_i. The EDL based REG controller can be pre-trained with the data of conventional generation dispatch and control. The pre-trained data contains high-quality data and low-quality data. Thus, the pre-trained data can cover all the state space, which is different from a conventional reinforcement learning [43, 44] (Fig. 7).

The next frequency deviation of the i-th cell $\Delta f_{i,(t+1)}$ can be predicted by the EDL from the current frequency deviation $\Delta f_{i,t}$, the current CCE $e_{i,t}$, and tested action set A_j. Generally, the current frequency and the current CCE are difficult to cover all the state space in a conventional simulation. However, in the pre-training process, the current frequency and the current CCE can be configured to any values. Besides, all the action vectors of the actions set A are simulated in the pre-training process. The control period of the EDL based REG controller is the same as the control period of the AGC process, i.e., 4 s. Therefore, all the state space can be covered by the EDL with the data of the inputs and the outputs of each control period (Fig. 7).

Table 2. Algorithms for the simulations of these two future smart grids

Number	UC/ED/GCD	AGC
1	Ant lion optimizer (ALO)	PID
2	Multi-verse optimizer (MVO)	Sliding mode controller (SMC)
3	Dragonfly algorithm (DA)	Active disturbance rejection control (ADRC)
4	Group search optimizer (GSO)	Fractional order PID (FOPID)
5	Chicken swarm optimization (CSO)	Fuzzy logic control (FLC)
6	Biogeography-based optimization (BBO)	Q learning
7	Moth-flame optimization (MFO)	Q(λ) learning
8	Whale optimization algorithm (WOA)	R(λ) learning
9	Simulated annealing algorithm (SAA)	
10	Genetic algorithm (GA)	
11	Grey wolf optimizer (GWO)	
12	Particle swarm optimization (PSO)	
13	Sine cosine algorithm (SCA)	
14	Ant colony optimization for continuous domains (ACOR)	
15	Teaching-learning-based optimization (TLBO)	
16	Firefly algorithm (FA)	
17	Imperialist competitive algorithm (ICA)	
18	Cultural algorithm (CA)	
19	Artificial bee colony (ABC)	
20	Invasive weed optimization (IWO)	
21	Strength Pareto evolutionary algorithm 2 (SPEA2)	
22	Covariance matrix adaptation evolution strategy (CMA-ES)	
23	Differential evolution (DE)	
24	Harmony search (HS)	
25	Shuffled complex evolution (SCE)	
26	Shuffled frog leaping algorithm (SFLA)	
27	Fixed proportion	
28	Expandable deep learning (EDL)	

5. Case studies

The configured simulation time of each CGC algorithm or REG controller is set to 24 hours or 86400 s in this paper. A total of 216 combined CGC algorithms (27 UC/ED/GCD algorithms $\times$ 8 AGC algorithms), and the EDL are simulated in two simulations, i.e., a 118-bus power system with 54 TSEs 5 cells, and a 13659-bus power system with a total of 4092 TSEs 10 cells (Table 2). Since these algorithms are simulated in these two future smart grids based on WoCs, the total configured simulation time of the simulations is 434 days or 2$\times$(27 $\times$ 8 +1) days. The configured control period of the REG controller or AGC is set to be 4 s in the following two cases. The optimization period of the UC programming, the ED programming, and the GCD programming are set to 24 hours, 15 minutes, and 4 seconds, respectively. The numbers of the inputs of the i-th cell of these cases are set to be $n_{\mathrm{i}} = 2$, i.e., frequency deviation Δf_i and CCE e_i. The coefficients of the hidden units of the EDL are set to be $n_1 = 2$, $n_2 = 3$, $n_3 = 3$, and $n_4 = 2$ in all cases.

5.1. A 118-bus power system with 54 three-state energies 5 cells

This case is developed on an AMAX XR-28201GK with double Core 12 Duo processor of 2.20 GHz and 96 GB RAM server in the MATLAB with version 9.3.0.713579 (R2017b).

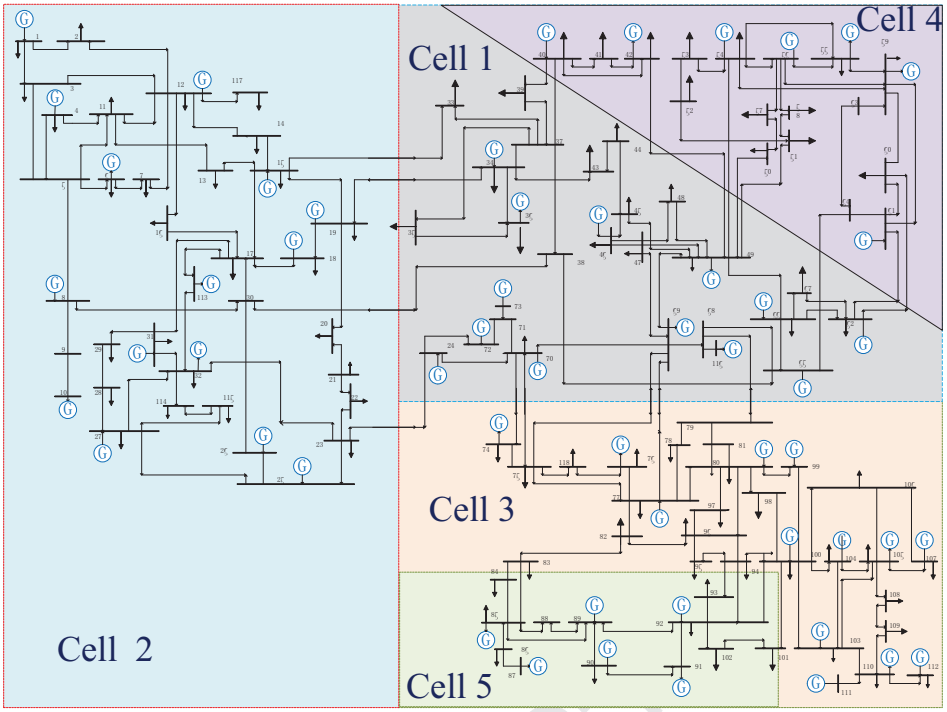

Fig. 8. Structure of the 118-bus power system with 54 three-state energies 5 cells

This case is based on the IEEE 118-bus 54-generation power system. This power system is divided into 5 cells, i.e., 'Cell 1', 'Cell 2', 'Cell 3', 'Cell 4', and 'Cell 5'. Besides, this power system contains 54 TSEs, i.e., three-state energies {24, 34, 36, 46, 49, 62, 65, 66, 69, 70, 72, 73, 116} for 'Cell 1', three-state energies {1, 4, 6, 8, 10, 12, 15, 18, 19, 25, 26, 27, 31, 32, 113} for 'Cell 2', three-state energies {74, 76, 77, 80, 99, 100, 103, 104, 105, 107, 110, 111, 112} for 'Cell 3', three-state energies {40, 42, 54, 55, 56, 59, 61} for 'Cell 4', and three-state energies {85, 87, 89, 90, 91, 92} for 'Cell 5' (Fig. 8). Each cell contains at least one generator, one inflexible load, one flexible load, one controllable wind power, one controllable photovoltaic power, and one plug-in hybrid electric vehicle (Fig. 9). The numbers of the outputs of all cells of this case are set to be $n_{\mathrm{o}} = \{13,\ 15,\ 13,\ 7,\ 6\}$. The wind power and photovoltaic power of all the cells of this web-of-cells are set to the same (Fig. 10(a)), while the inflexible load of each cell of this future smart grid is similar to each other (Fig. 10(b)). The parameters of this power system and the compared simulated methods are given in Appendix A.

The absolute mean value of the simulation result obtained by four combined conventional algorithms and the proposed EDL are shown as Fig. 11. These four combined conventional algorithms are the algorithms that obtain the optimal minimum frequency, minimum CCE, minimum cost, and minimum calculation time, respectively. The statistical absolute mean value of the simulation result obtained by all the conventional algorithms are given in Table 3.

Fig. 9 shows that: (i) the numbers of energies and system loads of the 118-bus power system in

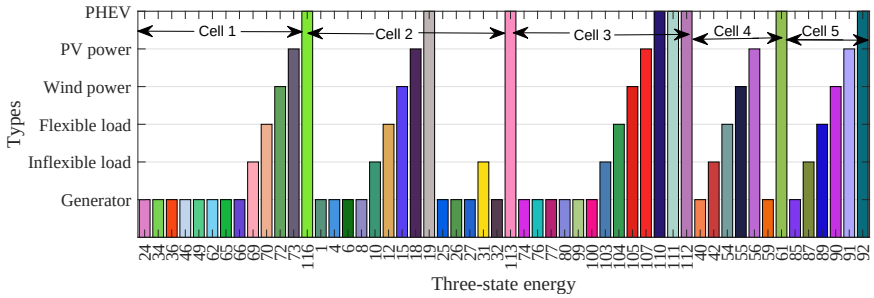

Fig. 9. Types of 54 three-state energies

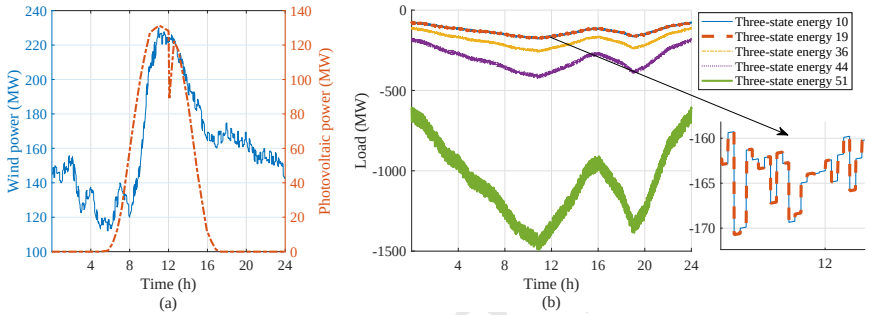

Fig. 10. Curves of some three-state energies: (a) wind power and photovoltaic power, (b) inflexible load

this case are fixed numbers; (ii) the numbers of the inputs and the outputs of the EDL based REG controllers of each cell in this 118-bus power system are fixed numbers; (iii) the topology of this power system is fixed topology. In Table 3, the 'Max satisfaction (%)' means the statistical satisfaction of multiple objectives, and the statistical satisfaction of the j-th compared method can be calculated as follows,

$$\eta_{j,\text{total}} = 1 - \frac{1}{n_{\text{objective}}} \sum_{i=1}^{n_{\text{objective}}} \frac{o_{j,i}}{o_{\text{max},i}} \tag{9}$$

where $n_{\text{objective}}$ is the number of objectives; and it is set to be $n_{\text{objective}}$=4 in this paper, i.e., cost objective, frequency deviation objective, the CCE objective, and calculation time objective; thus, the range of the variable i is set to $i = \{1,\ 2,\ 3,\ 4\}$; $o_{j,i}$ is the i-th objective value of the j-th compared method; $o_{\text{max},i}$ is the maximum objective value in the i-th objective values of all the compared methods; the range of the variable j is set to $j = \{1,\ 2,\ ...,\ n_{\text{method}}\}$, and n_{method} is set to 217 (or 216 combined CGC algorithms and the proposed EDL); therefore, the larger statistical satisfaction $\eta_{j,\text{total}}$ means the higher control performance.

In Fig. 11, the '1- Max satisfaction' $(1 - \eta_{j,\text{total}})$ is shown. The larger statistical satisfaction means the smaller $1 - \eta_{j,\text{total}}$, and then means higher control performance. Therefore, the smaller indices in Fig. 11 means the higher control performance; and the nearer indices points to the center of Fig. 11 means the higher control performance.

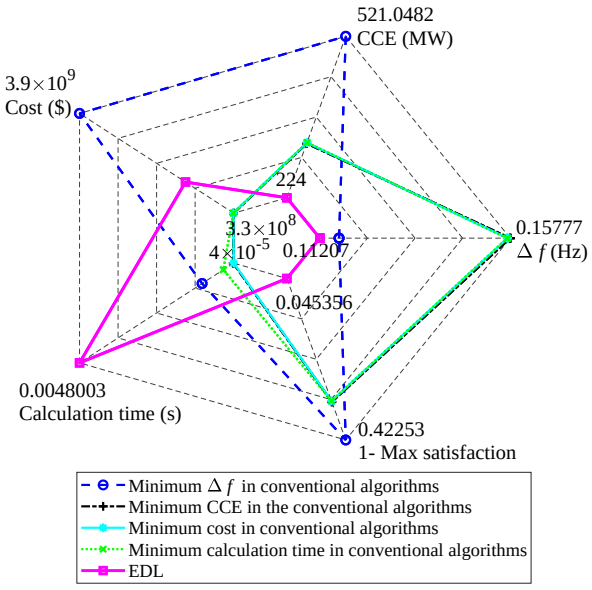

Fig. 11. Results of the 118-bus power system with 54 three-state energies 5 cells

Fig. 11 and Table 3 show that: (i) one conventional combined algorithm can obtain smaller cost objective with larger frequency deviation and CCE; (ii) one conventional combined algorithm can obtain smaller frequency deviation with larger cost objective; (iii) the average calculation time used by the EDL based REG controller is larger than the average calculation time used by a part of conventional combined algorithms; (iv) the maximum calculation time used by the EDL based REG controller is far less than the control period (0.0066 s $<<$ 4 s); while the maximum calculation time used by conventional combined algorithms is larger than the control period (5.69 s $>$ 4 s).

The simulation results (Fig. 11 and Table 3) obtained by the CGC controller and the EDL based controller show that:

(1) Compared with the CGC controller, the EDL based REG controller can obtain the highest control performance with smaller frequency deviation Δf_i and CCE e_i.

(2) Since the unified generation commands for TSEs can be obtained from the EDL based REG controller, the TSEs of future smart grids can be effectively controlled by the EDL based REG controller.

5.2. A 13659-bus power system with a total of 4092 three-state energies 10 cells with varying topology

This case is developed on an AMAX Intel(R) Xeon(R) Platinum 8160 CPU with double Core 24 Duo processor of 2.10 GHz and 192 GB RAM server in the MATLAB with version 9.3.0.713579 (R2017b).

Table 3. Statistics results of the 118-bus power system with 54 three-state energies 5 cells

Objective	Conventional algorithms			EDL		
	Min.	Mean	Max.	Min.	Mean	Max.
Δf (Hz)	0.0147	0.1392	1.5705	0.0186	0.1121	0.6613
CCE (MW)	0.0095	425.7182	2631.8567	0.0156	224.9782	1164.7807
Cost ($)	3.33×10^8	2.31×10^9	6.51×10^9	–	1.45×10^9	–
Calculation time (s)	5.94×10^{-5}	0.62	5.69	0.0027	0.0048	0.0066
Max satisfaction (%)	33.33	57.11	66.85	–	95.46	–

This case is based on the 13659-bus 4092-generation power system from the MATPOWER with version 6.0 and later. This case representing parts of the European high voltage transmission network, stemming from the *Pan European Grid Advanced Simulation and State Estimation* project [45]. This power system is divided to 10 cells, and the maximum numbers of all TSEs of these 10 cells are {319, 278, 558, 579, 136, 357, 324, 471, 517, 553}. Therefore, the numbers of the outputs of all cells of this case are set to be $n_{\mathrm{o}} = \{319, 278, 558, 579, 136, 357, 324, 471, 517, 553\}$. The compared algorithms for all the 10 cells in this case are simulated in 10 independent processors with parallel simulation. The network topology of this case is a varying topology (Fig. 12). The total numbers of TSEs in the future smart grid are 3265, 3656, 4092, and 3656 at the time 'From 0 to 6 h', 'From 7 h to 12 h', 'From 13 h to 18 h', and 'From 19 h to 24 h', respectively.

Fig. 12 shows that: (i) the number of the TSEs in the future smart grid can increased and decreased, then the parameters of the controller for these TSEs should be updated with the varying future smart grid; (ii) the power system in this case is a large interconnected power system with varying topology; and the topology of the future smart grid can be expanded and contracted; (iii) the topology of the future smart grid may more frequent expanded or contracted in a real power system; (iv) to compared with the control performance of the EDL based REG controller, the parameters of the 216 compared combined conventional algorithms should be re-configured at each six simulated hours; thus, these parameters are re-configured at the simulated time of 0 s, 21600 s, 43200 s, and 64800 s. The parameters of the generators types of TSEs in this power system are repeat vectors from that the 118-bus power system with 54 three-state energies 5 cells. The parameters of the compared simulated methods of this power system are the same as that of the 118-bus power system with 54 three-state energies 5 cells.

Fig. 12 and Table 4 show that: (i) the EDL based REG controller obtains the optimal cost

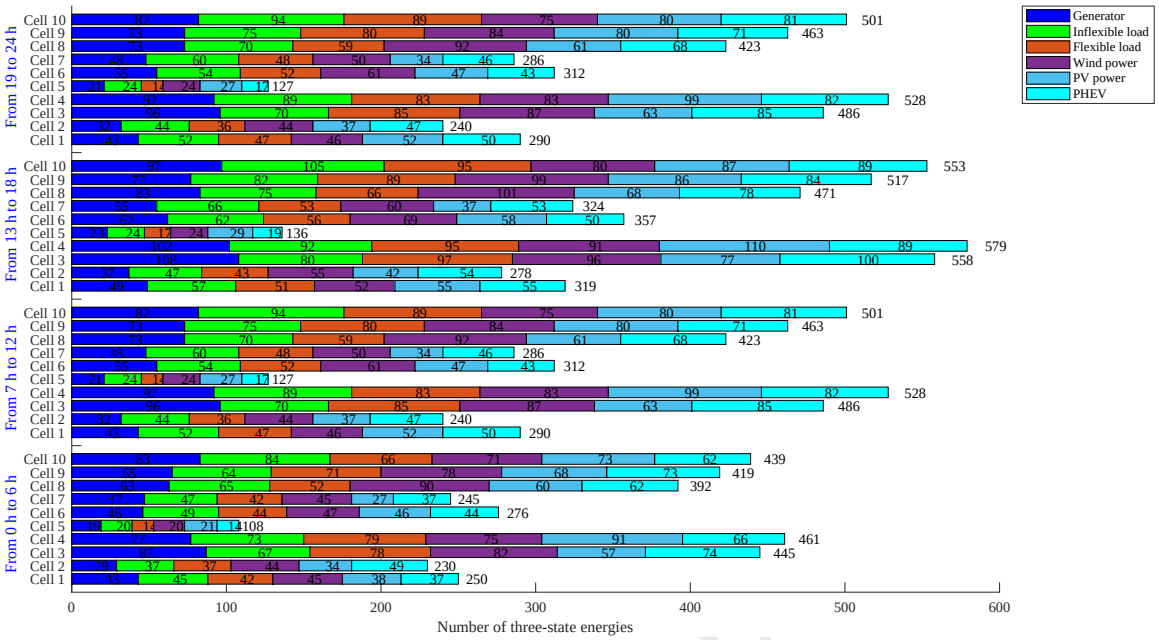

Fig. 12. Types of maximum 4092 three-state energies

objective, CCE, and frequency deviation, and maximum satisfaction value; (ii) compared with conventional combined algorithms, the EDL based REG controller can obtain multiple objectives simultaneously; (iii) the maximum calculation time used by the EDL based REG controller is far less than the control period (0.44118 s << 4 s); (iv) in Fig. 12 and Fig. 11, the control performances of five methods are compared, i.e., the EDL based REG controller, and four other combined conventional algorithms; these four other combined conventional algorithms are the method that can obtain minimum frequency deviation in the 216 compared combined conventional algorithms, the method that can obtain minimum CCE in the 216 compared combined conventional algorithms, the method that can obtain minimum cost in the 216 compared combined conventional algorithms, and the method that used minimum calculation time in the 216 compared combined conventional algorithms.

The simulation results (Fig. 13 and Table 4) obtained by the CGC controller and the EDL controller show that:

(1) Compared with the CGC controller, the EDL based REG controller can obtain the highest control performance with smaller frequency deviation Δf_i and CCE e_i in a complex future smart grid based on WoCs.

(2) Since the maximum calculation time used by the EDL (0.44118 s) is much less than the control period (4 s), the future smart grid can be effectively controlled by the EDL based REG controller.

(3) With the expandable ability of the EDL, the EDL based controller can effectively provide varying outputs to all the cells of the future smart grid. Compared with relaxed deep learning, the

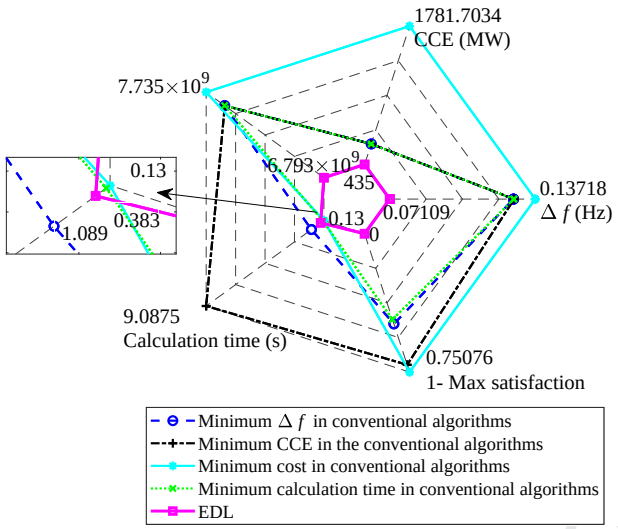

Fig. 13. Result of the 13659-bus power system with a total of 4092 three-state energies 10 cells with varying topology

Table 4. Statistics results of the 13659-bus power system with a total of 4092 three-state energies 10 cells with varying topology

Objective	Conventional algorithms			EDL		
	Min.	Mean	Max.	Min.	Mean	Max.
Δf (Hz)	0.0074481	0.12929	0.30791	0.007949	0.12736	0.29377
CCE (MW)	94.4687	779.8118	3385.5548	217.5372	635.9364	1222.0156
Cost ($)	7.586×10^9	7.611×10^9	7.735×10^9	–	7.588×10^9	–
Calculation time (s)	0.33334	0.41024	1.4428	0.37646	0.38294	0.44118
Max satisfaction (%)	0	62.6731	74.8229	–	99.5271	–

expandable deep learning can be applied into future smart grid with varying topology, while relaxed deep learning can only employed into a power system with fixed topology.

6. Conclusions

This paper proposes an expandable deep learning for future smart grids based on Web-of-Cells with three-state energies. Firstly, the real-time economic generation dispatch and control framework with unified time scale for future smart grids is built in this paper. Secondly, the concept of three-state energies is proposed for the prosumers of future smart grids. Last but least, an expandable deep learning approach is proposed for the real-time economic generation dispatch and controller of future smart grids in this paper. The simulations results under a 118-bus power system with 54 three-state

energies 5 cells and a 13659-bus power system with a total of 4092 three-state energies 10 cells with varying topology, verify the effectiveness and feasibility of the proposed expandable deep learning for the real-time economic generation dispatch and controller of future smart grids. The major features of the expandable deep learning based real-time economic generation dispatch and controller for three-state energies based future smart grids can be summarized as follows,

(1) Since the expandable deep learning can simultaneously provide multiple generation commands, the expandable deep learning based real-time economic generation dispatch and controller can simultaneously control all the three-state energies of future smart grids.

(2) Compared with the framework of conventional conventional generation dispatch and control, the combined processes of unit commitment, economic dispatch, automatic generation control, and, generation commands dispatch are replaced by the framework of real-time economic generation dispatch and control. Compared with previous work, which is relaxed deep learning algorithm for real-time economic generation dispatch and controller, the numbers of the inputs and the outputs of the relaxed deep learning are fixed numbers, while the numbers of the inputs and the outputs of the proposed expandable deep learning are varying numbers. With the expandable ability of the expandable deep learning, the expandable deep learning based controller can effectively provide varying outputs for future smart grids.

(3) Compared with previous relaxed deep learning algorithm, the topology of a power grid based on the relaxed deep learning algorithm should be fixed topology; while the topology of a future smart grid based on the proposed expandable deep learning can be varying topology. The expandable deep learning based real-time economic generation dispatch and controller can provide the optimal actions for the three-state energies based future smart grids with varying topology.

In the future smart grids, the expandable deep learning based real-time economic generation dispatch and controller should be improved when the real-time responses between demand side and generator side are considered. Besides, a coordinated expandable deep learning algorithm based on game theory should be considered when a cell of the Web-of-Cells game with other cells of the Web-of-Cells security with the point of view of game theory. Furthermore, a more global coordinated expandable deep learning algorithm should be considered with the development of spot electricity market in the view of the maximization of social welfare in the future smart grids.

7. Acknowledgment

The authors gratefully acknowledge the support of the National Natural Science Foundation of China (NSFC) (51777078) and Innovation Project of Guangxi Graduate Education (YCSW2019025).

Appendix A. Parameters of 118-bus power system with 54 three-state energies 5 cells and the compared simulated methods

Appendix A.1. Parameters of 118-bus power system with 54 three-state energies 5 cells

The initial running time of the generators types of TSEs for UC optimization: 8 hours;
the minimum continuous time of start-up state of the generators types of TSEs for UC optimization: 8 hours;
the minimum continuous time of closed state of the generators types of TSEs for UC optimization: 3 hours;
the time slots for UC optimization: 24 hours;
the maximum active power of the generators types of TSEs {24, 34, 36, 46, 49, 62, 65, 66, 1, 4, 6, 8, 25, 26, 27, 32, 74, 76, 77, 80, 99, 100, 40, 59, 85}:{455, 455, 130, 130, 162, 80, 85, 55, 55, 55, 455, 455, 130, 130, 162, 80, 85, 55, 55, 55, 455, 455, 130, 130, 162} MW;
the minimum active power of the generators types of TSEs: {150, 150, 20, 20, 25, 20, 25, 10, 10, 10, 150, 150, 20, 20, 25, 20, 25, 10, 10, 10, 150, 150, 20, 20, 25} MW;
the maximum and the minimum active power of the PHEV types of TSEs:10000, and -10000 MW, respectively;
the predicted inflexible load of each time slot: {700, 750, 850, 950, 1000, 1100, 1150, 1200, 1300, 1400, 1450, 1500, 1400, 1300, 1200, 1050, 1000, 1100, 1200, 1400, 1300, 1100, 900, 800} MW;
the quadratic square coefficients and the line coefficients of the generators types of TSEs for unit commitment and economic dispatch: {1000, 970, 700, 680, 450, 370, 480, 660, 665, 670, 1000, 970, 700, 680, 450, 370, 480, 660, 665, 670, 1000, 970, 700, 680, 450}, and {16.19, 17.26, 16.60, 16.50, 19.70, 22.26, 27.74, 25.92, 27.27, 27.79, 16.19, 17.26, 16.60, 16.50, 19.70, 22.26, 27.74, 25.92, 27.27, 27.79, 16.19, 17.26, 16.60, 16.50, 19.70};
the generation rate constraints for the generator types of TSEs: 200 MW/h.

Appendix A.2. Parameters of the compared simulated methods

PID:proportional k_{P}=-0.006031543250198, integral k_{I}=0.00043250;
SMC:switch on/off point $k_{\mathrm{p}} = \pm 0.1$Hz, output when on/off $k_{\mathrm{v}}\pm$=80 (MW);

ADRC: extended state observer $A = \begin{bmatrix} 0 & 0.0001 & 0 & 0 \\ 0 & 0 & 0.0001 & 0 \\ 0 & 0 & 0 & 0.0001 \\ 0 & 0 & 0 & 0 \end{bmatrix}$,

$B = \begin{bmatrix} 0 & 0 \\ 0 & 0 \\ 0.0001 & 0.0001 \\ 0 & 0 \end{bmatrix}$, $C = \text{diag}\begin{pmatrix} 0.1 & 0.1 & 0.1 & 0.1 \end{pmatrix}$, $D = \mathbf{0}_{4\times 2}$, k_1=15.0, k_2=5.5, k_3=2.0, k_4=1;

FOPID: proportional k_{P}=-1, integral k_{I}=0.43250, λ=1.3, μ=200 ;

FLC: X (input, Δf) 21 grids from -0.2 to 0.2 (Hz), Y (input, $\int \Delta f$) 21 grids from -1 to 1 (Hz), Z (output, ΔP) is 441 grids from -150 to 150 (MW);

Q learning: actions set A={-300,-240,-180,-120, -60, 0, 60, 120, 180, 240, 300}, learning rate α=0.1, the constant of probability distribution method β=0.5, the discounted rate of future reward γ=0.9;

Q(λ) learning: A={-300,-240,-180,-120, -60, 0, 60, 120, 180, 240, 300}, α=0.1, β=0.5, γ=0.9, λ=0.9;

R(λ) learning: A={-300,-240,-180,-120, -60, 0, 60, 120, 180, 240, 300}, α=0.1, β=0.5, γ=0.9, λ=0.9, R_0=0;

All the optimization algorithms for UC: number of generations N_{g}=100, population size P_{s}=100;

All the optimization algorithms for ED: N_{g}=30, P_{s}=50;

All the optimization algorithms for GCD: N_{g}=30, P_{s}=50;

Fixed proportion for GCD:$k_j = \frac{\Delta P_j^{\max}}{\sum \Delta P_j^{\max}} \Delta P_j$,$j = 1, 2, ..., J_i$,i=1,2,...,3.

References

[1] L. Liu, T. Zhu, Y. Pan, H. Wang, Multiple energy complementation based on distributed energy systems - case study of chongming county, china, Applied Energy 192 (2017) 329–336.

[2] L. Yin, T. Yu, X. Zhang, B. Yang, Relaxed deep learning for real-time economic generation dispatch and control with unified time scale, Energy 149 (2018) 11 – 23.

[3] E. Mayhorn, L. Xie, K. Butler-Purry, Multi-time scale coordination of distributed energy resources in isolated power systems, IEEE Transactions on Smart Grid 8 (2) (2017) 998–1005.

[4] X. Peng, X. Tao, Cooperative game of electricity retailers in china's spot electricity market, Energy 145 (2018) 152 – 170.

[5] M. Rahman, A. Oo, Distributed multi-agent based coordinated power management and control strategy for microgrids with distributed energy resources, Energy Conversion and Management 139 (2017) 20 – 32.

[6] S. Zhang, R. Xiong, F. Sun, Model predictive control for power management in a plug-in hybrid electric vehicle with a hybrid energy storage system, Applied Energy 185 (2017) 1654 – 1662.

[7] J. Peng, H. He, R. Xiong, Rule based energy management strategy for a series-parallel plug-in hybrid electric bus optimized by dynamic programming, Applied Energy 185 (2017) 1633 – 1643.

[8] X. Xing, J. Lin, C. Wan, Y. Song, Model predictive control of lpc-looped active distribution network with high penetration of distributed generation, IEEE Transactions on Sustainable Energy 8 (3) (2017) 1051–1063.

[9] S. Tabatabaee, S. S. Mortazavi, T. Niknam, Stochastic scheduling of local distribution systems considering high penetration of plug-in electric vehicles and renewable energy sources, Energy 121 (2017) 480 – 490.

[10] Y. Li, B. Feng, G. Li, J. Qi, D. Zhao, Y. Mu, Optimal distributed generation planning in active distribution networks considering integration of energy storage, Applied Energy 210 (2018) 1073 – 1081.

[11] G. Mokryani, Y. F. Hu, P. Papadopoulos, T. Niknam, J. Aghaei, Deterministic approach for active distribution networks planning with high penetration of wind and solar power, Renewable Energy 113 (2017) 942 – 951.

[12] Y. Chai, L. Guo, C. Wang, Z. Zhao, X. Du, J. Pan, Network partition and voltage coordination control for distribution networks with high penetration of distributed pv units, IEEE Transactions on Power Systems 33 (3) (2018) 3396–3407.

[13] C. Tornelli, R. Zuelli, M. Marinell, A. Z. Morch, L. Cornez, Requirements for future control room and visualisation features in the Web-of-Cells framework defined in the ELECTRA project, CIRED - Open Access Proceedings Journal 2017 (1) (2017) 1425–1428.

[14] L. Cheng, T. Yu, Exploration and exploitation of new knowledge emergence to improve the collective intelligent decision-making level of web-of-cells with cyber-physical-social systems based on complex network modeling, IEEE Access 6 (2018) 74204–74239.

[15] B. M. Delgado, S. Cao, A. Hasan, K. Sirn, Thermoeconomic analysis of heat and electricity prosumers in residential zero-energy buildings in finland, Energy 130 (2017) 544 – 559.

[16] D. Zou, S. Li, Z. Li, X. Kong, A new global particle swarm optimization for the economic emission dispatch with or without transmission losses, Energy Conversion and Management 139 (2017) 45 – 70.

[17] Y. Arya, Agc performance enrichment of multi-source hydrothermal gas power systems using new optimized fofpid controller and redox flow batteries, Energy 127 (2017) 704 – 715.

[18] S. D. Beigvand, H. Abdi, M. L. Scala, A general model for energy hub economic dispatch, Applied Energy 190 (2017) 1090 – 1111.

[19] L. Xi, T. Yu, B. Yang, X. Zhang, X. Qiu, A wolf pack hunting strategy based virtual tribes control for automatic generation control of smart grid, Applied Energy 178 (2016) 198 – 211.

[20] K. Nghitevelekwa, R. Bansal, A review of generation dispatch with large-scale photovoltaic systems, Renewable and Sustainable Energy Reviews 81 (2018) 615 – 624.

[21] T. Levin, J. Kwon, A. Botterud, The long-term impacts of carbon and variable renewable energy policies on electricity markets, Energy Policy 131 (2019) 53 – 71.

[22] R. Zafar, A. Mahmood, S. Razzaq, W. Ali, U. Naeem, K. Shehzad, Prosumer based energy management and sharing in smart grid, Renewable and Sustainable Energy Reviews 82 (2018) 1675 – 1684.

[23] S. Y. Abujarad, M. Mustafa, J. Jamian, Recent approaches of unit commitment in the presence of intermittent renewable energy resources: A review, Renewable and Sustainable Energy Reviews 70 (2017) 215 – 223.

[24] V. Bhattacharjee, I. Khan, A non-linear convex cost model for economic dispatch in microgrids, Applied Energy 222 (2018) 637 – 648.

[25] X. S. Zhang, Q. Li, T. Yu, B. Yang, Consensus transfer Q-learning for decentralized generation command dispatch based on virtual generation tribe, IEEE Transactions on Smart Grid 9 (3) (2018) 2152–2165.

[26] N. Zhang, Z. Hu, D. Dai, S. Dang, M. Yao, Y. Zhou, Unit commitment model in smart grid environment considering carbon emissions trading, IEEE Transactions on Smart Grid 7 (1) (2016) 420–427.

[27] Z. Yang, X. Ji, Y. Li, Distributed consensus based supply-demand balance algorithm for economic dispatch problem in a smart grid with switching graph, IEEE Transactions on Industrial Electronics 64 (2) (2017) 1600–1610.

[28] B. Wang, J. Xu, B. Cao, B. Ning, Adaptive mode switch strategy based on simulated annealing optimization of a multi-mode hybrid energy storage system for electric vehicles, Applied Energy 194 (2017) 596 – 608.

[29] A. Fathy, H. Rezk, Multi-verse optimizer for identifying the optimal parameters of PEMFC model, Energy 143 (2018) 634 – 644.

[30] S. M. Ebrahimi, E. Salahshour, M. Malekzadeh, F. Gordillo, Parameters identification of pv solar cells and modules using flexible particle swarm optimization algorithm, Energy 179 (2019) 358 – 372.

[31] M. A. Memon, S. Mekhilef, M. Mubin, M. Aamir, Selective harmonic elimination in inverters using bio-inspired intelligent algorithms for renewable energy conversion applications: A review, Renewable and Sustainable Energy Reviews 82 (2018) 2235 – 2253.

[32] H. Ma, Z. Yang, P. You, M. Fei, Multi-objective biogeography-based optimization for dynamic economic emission load dispatch considering plug-in electric vehicles charging, Energy 135 (2017) 101 – 111.

[33] G. Kan, M. Zhang, K. Liang, H. Wang, Y. Jiang, J. Li, L. Ding, X. He, Y. Hong, D. Zuo, Z. Bao, C. Li, Improving water quantity simulation & forecasting to solve the energy-water-food nexus issue by using heterogeneous computing accelerated global optimization method, Applied Energy 210 (2018) 420 – 433.

[34] L. Xiao, W. Shao, T. Liang, C. Wang, A combined model based on multiple seasonal patterns and modified firefly algorithm for electrical load forecasting, Applied Energy 167 (2016) 135 – 153.

[35] M. Z. Ali, P. N. Suganthan, R. G. Reynolds, A. F. Al-Badarneh, Leveraged neighborhood restructuring in cultural algorithms for solving real-world numerical optimization problems, IEEE Transactions on Evolutionary Computation 20 (2) (2016) 218–231.

[36] M. Mao, L. Zhang, P. Duan, Q. Duan, M. Yang, Grid-connected modular PV-converter system with shuffled frog leaping algorithm based DMPPT controller, Energy 143 (2018) 181 – 190.

[37] Y. Li, S. Tong, Adaptive fuzzy control with prescribed performance for block-triangular-structured nonlinear systems, IEEE Transactions on Fuzzy Systems 26 (3) (2018) 1153–1163.

[38] A. Chevalier, C. Francis, C. Copot, C. M. Ionescu, R. D. Keyser, Fractional-order pid design: Towards transition from state-of-art to state-of-use, ISA Transactions 84 (2019) 178 – 186.

[39] F. Alonge, M. Cirrincione, F. DIppolito, M. Pucci, A. Sferlazza, Robust active disturbance rejection control of induction motor systems based on additional sliding-mode component, IEEE Transactions on Industrial Electronics 64 (7) (2017) 5608–5621.

[40] X. S. Zhang, T. Yu, Z. N. Pan, B. Yang, T. Bao, Lifelong learning for complementary generation control of interconnected power grids with high-penetration renewables and EVs, IEEE Transactions on Power Systems 33 (4) (2018) 4097–4110.

[41] M. Vahid-Pakdel, S. Nojavan, B. Mohammadi-ivatloo, K. Zare, Stochastic optimization of energy hub operation with consideration of thermal energy market and demand response, Energy Conversion and Management 145 (2017) 117 – 128.

[42] J. Yoon, E. Yang, J. Lee, S. J. Hwang, Lifelong learning with dynamically expandable networks, arXiv preprint arXiv:1708.01547 (2017) 1–10.

[43] L. Xi, J. Chen, Y. Huang, Y. Xu, L. Liu, Y. Zhou, Y. Li, Smart generation control based on multi-agent reinforcement learning with the idea of the time tunnel, Energy 153 (2018) 977 – 987.

[44] H. Kazmi, F. Mehmood, S. Lodeweyckx, J. Driesen, Gigawatt-hour scale savings on a budget of zero: Deep reinforcement learning based optimal control of hot water systems, Energy 144 (2018) 159 – 168.

[45] C. Josz, S. Fliscounakis, J. Maeght, P. Panciatici, AC power flow data in MATPOWER and QCQP format: iTesla, RTE snapshots, and PEGASE, arxiv.org arXiv (arXiv:1603.01533) (2016) 1–7.

Highlights (for review)

- Three-state energy model is proposed for Web-of-Cells based future smart grid (FSG).
- The inputs and outputs of expandable deep learning (EDL) can be expanded dynamically.
- EDL based real-time economic generation controller (RGC) is proposed.
- Varying three-state energies of the FSG can be controlled by the EDL controller.
- RGC obtain highest control performance for FSG with varying topology effectively.